CrossMark

Reflection of plane waves from the boundary of an incompressible finitely deformed electroactive half-space

Baljeet Singh and Ray W. Ogden

Abstract. Within the framework of the quasi-electrostatic approximation, the theory of the superposition of infinitesimal deformations and electric fields on a finite deformation with an underlying electric field is employed to examine the problem of the reflection of small amplitude homogeneous electroelastic plane waves from the boundary of an incompressible finitely deformed electroactive half-space. The theory is applied to the case of two-dimensional incremental motions and electric fields with an underlying biasing electric field normal to the half-space boundary, and the general incremental governing equations are obtained for this specialization. For illustration, the equations are then applied to a simple prototype electroelastic model for which it is found that only a single reflected wave is possible and a surface wave is in general generated for each angle of incidence. Explicit formulas are obtained for the wave speed and the reflection and surface wave coefficients in terms of the deformation, magnitude of the electric (displacement) field, the electromechanical coupling parameters, and the angle of incidence, and the results are illustrated graphically.

Mathematics Subject Classification. 74B15, 74B20, 74F15, 74J05, 74J15.

Keywords. Nonlinear electroelasticity, Electroelastic plane waves, Reflection of plane waves, Surface waves.

1. Introduction

The general nonlinear theory of electroelasticity is concerned with the coupling between the electric and the mechanical properties of materials such as electroactive elastomers, which are capable of large deformations. In the present paper, we consider a problem of the reflection of plane waves from the boundary of a finitely deformed incompressible electroactive half-space with a biasing electric field normal to the half-space boundary. This is based on the form of the theory of electromechanical interactions as developed by Dorfmann and Ogden [1] and the theory of the propagation of small amplitude waves in a nonlinear electroelastic material within the quasi-electrostatic approximation, as in [2]. The counterpart of the current analysis for a purely elastic material was examined by Ogden and Sotiropoulos [3], while a small number of papers have considered the propagation and reflection of small amplitude waves in the presence of initial stress and/or biasing fields. For example, Liu et al. [4] studied the effects of pre-stress on the propagation of waves of Bleustein–Gulyaev type in piezoelectric materials, Simionescu-Panait [5] examined the effect of electrostriction on the propagation of plane waves in an isotropic solid subjected to small initial fields, and Singh [6] studied the effect of initial stress on the reflection coefficients at the boundary of a piezoelectric half-space. See also the review of electroelastic waves under biasing fields by Yang and Hu [7].

In Sects. 2, 3, and 4, the general theory of electroelasticity and its incremental counterpart are reviewed briefly. In Sect. 5, the equations and boundary conditions are specialized to two-dimensional increments for a plane strain underlying configuration and for an illustrative prototype electroelastic material model. The equations governing the propagation of plane waves are then given in Sect. 6 and applied in Sect. 7 to the problem of reflection of plane waves, as indicated above. For the considered material model, it is found that for each angle of incidence only a single reflected wave exists, and this is in general accompanied

Birkhäuser

by the generation of a surface wave. Explicit expressions are obtained for the speed of plane waves, and the reflection and surface wave coefficients, which in general depend on the deformation, magnitude of the electric (displacement) field, electromechanical coupling parameters, and the angle of incidence. The dependence is illustrated graphically in Sect. 8, and some concluding remarks are provided in Sect. 9.

2. The basic equations of nonlinear electroelasticity

We denote by $\mathcal{B}_r$ a fixed reference configuration of a continuous electroelastic body in the absence of mechanical loads and electric fields. Material points in $\mathcal{B}_r$ are labeled by their position vectors $\mathbf{X}$. Let the motion of the body be described by the equation $\mathbf{x} = \chi(\mathbf{X}, t)$, where t is time and the vector function χ is defined for all points $\mathbf{X}$ in $\mathcal{B}_r$, $\mathbf{x}$ being the position of the material point $\mathbf{X}$ in the current configuration of the body, denoted $\mathcal{B}_t$ at time t. The configuration $\mathcal{B}_t$ is in general maintained by a combination of mechanical loads and an electric field vector, denoted $\mathbf{E}$, which is associated with the electric displacement vector, denoted $\mathbf{D}$. We refer to the book [8] for details of the relevant equations from nonlinear continuum mechanics and to [9] for a general treatment of nonlinear electromechanical coupling.

In the present study, we neglect the magnetic field and electromagnetic interactions and adopt the quasi-electrostatic approximation. Then, in the absence of free body charges and currents, Maxwell's equations specialize to

$$\text{curl}\,\mathbf{E} = \mathbf{0}, \quad \text{div}\,\mathbf{D} = 0, \tag{1}$$

where curl and div are curl and divergence operators with respect to $\mathbf{x}$. Readers are referred to the classic text [10] for details of the equations of electromagnetic theory.

Let $\mathbf{E}_L$ and $\mathbf{D}_L$ be the Lagrangian counterparts of $\mathbf{E}$ and $\mathbf{D}$, respectively. These are defined by

$$\mathbf{E}_L = \mathbf{F}^T\mathbf{E}, \quad \mathbf{D}_L = J\mathbf{F}^{-1}\mathbf{D}, \tag{2}$$

where $\mathbf{F} = \text{Grad}\,\chi$ is the deformation gradient, with Grad being the gradient operator in B_r, ^{T} the usual transpose operator and $J = \det \mathbf{F}$. For incompressible materials, on which we focus in the article, the constraint

$$J = \det \mathbf{F} \equiv 1 \tag{3}$$

applies for each $\mathbf{X}$.

Using Eq. (2), the equations in (1) can be written in Lagrangian form as

$$\text{Curl}\,\mathbf{E}_L = \mathbf{0}, \quad \text{Div}\,\mathbf{D}_L = 0, \tag{4}$$

where Curl and Div are the curl and divergence operators in $\mathcal{B}_r$.

In the absence of mechanical body forces, the equation of motion of the material can be written as

$$\text{div}\,\boldsymbol{\tau} = \rho\mathbf{x}_{,tt}, \tag{5}$$

where $\boldsymbol{\tau}$ is the total Cauchy stress tensor, which is symmetric, and ρ is the mass density of the material in $\mathcal{B}_t$. A subscript t following a comma denotes the material time derivative.

The total nominal stress tensor $\mathbf{T}$ is defined, for an incompressible material, by

$$\mathbf{T} = \mathbf{F}^{-1}\boldsymbol{\tau}. \tag{6}$$

Using (6), Eq. (5) is written in Lagrangian form as

$$\text{Div}\,\mathbf{T} = \rho_r\mathbf{x}_{,tt}, \tag{7}$$

where ρ_r is mass density in $\mathcal{B}_r$, which, since we are considering incompressible materials, is equal to ρ, and henceforth the subscript r is omitted from ρ_r.

We consider an energy function Ω^*, defined per unit volume in $\mathcal{B}_r$ as a function of $\mathbf{F}$ and $\mathbf{D}_L$. Then, for an incompressible material the total nominal stress tensor and the Lagrangian electric field are given by

$$\mathbf{T} = \frac{\partial \Omega^*}{\partial \mathbf{F}} - p\mathbf{F}^{-1}, \quad \mathbf{E}_L = \frac{\partial \Omega^*}{\partial \mathbf{D}_L}, \tag{8}$$

where p is a Lagrange multiplier associated with incompressibility constraint (3), and hence

$$\boldsymbol{\tau} = \mathbf{F}\frac{\partial \Omega^*}{\partial \mathbf{F}} - p\mathbf{I}, \quad \mathbf{E} = \mathbf{F}^{-T}\frac{\partial \Omega^*}{\partial \mathbf{D}_L}, \tag{9}$$

where $\mathbf{I}$ is the identity tensor.

For an incompressible isotropic electroelastic material, Ω^* can be written in terms of five scalar invariants of the two tensors $\mathbf{C}$ and $\mathbf{D}_L \otimes \mathbf{D}_L$, where $\mathbf{C}$ is the right Cauchy–Green tensor, defined as $\mathbf{F}^T\mathbf{F}$. The invariants typically adopted are defined as

$$I_1 = \operatorname{tr}\mathbf{C}, \quad I_2 = \frac{1}{2}[(\operatorname{tr}\mathbf{C})^2 - \operatorname{tr}(\mathbf{C}^2)], \tag{10}$$

$$I_4 = \mathbf{D}_L \cdot \mathbf{D}_L, \quad I_5 = \mathbf{D}_L \cdot (\mathbf{C}\mathbf{D}_L), \quad I_6 = \mathbf{D}_L \cdot (\mathbf{C}^2\mathbf{D}_L). \tag{11}$$

It follows that $\boldsymbol{\tau}$ and $\mathbf{E}$ can be expanded in the forms

$$\boldsymbol{\tau} = 2\Omega_1^*\mathbf{B} + 2\Omega_2^*\left(I_1\mathbf{B} - \mathbf{B}^2\right) - p\mathbf{I} + 2\Omega_5^*\mathbf{D} \otimes \mathbf{D} + 2\Omega_6^*(\mathbf{D} \otimes \mathbf{BD} + \mathbf{BD} \otimes \mathbf{D}), \tag{12}$$

$$\mathbf{E} = 2\left(\Omega_4^*\mathbf{B}^{-1} + \Omega_5^*\mathbf{I} + \Omega_6^*\mathbf{B}\right)\mathbf{D}, \tag{13}$$

where $\mathbf{B} = \mathbf{FF}^T$ is the left Cauchy–Green tensor, Ω_i^* is defined as $\partial\Omega^*/\partial I_i$ for $i = 1, 2, 4, 5, 6$, and we now use the notation $\Omega^* = \Omega^*(I_1, I_2, I_4, I_5, I_6)$.

3. Incremental motions and electric fields

Consider a static finite deformation $\mathbf{x} = \boldsymbol{\chi}(\mathbf{X})$, which defines a deformed configuration $\mathcal{B}$ with deformation gradient $\mathbf{F}$, electrostatic displacement field $\mathbf{D}$, corresponding Lagrangian field $\mathbf{D}_L = \mathbf{F}^{-1}\mathbf{D}$ and electric field $\mathbf{E} = \mathbf{F}^{-T}\mathbf{E}_L$ given by $(8)_2$. Upon this configuration, we superimpose a small (incremental) time-dependent displacement $\dot{\mathbf{x}}(\mathbf{X}, t)$, where here and henceforth a superposed dot signifies an incremental quantity. The associated incremental deformation gradient is given by $\dot{\mathbf{F}} = \operatorname{Grad}\dot{\mathbf{x}}$. Independently of $\dot{\mathbf{x}}$, we suppose that $\dot{\mathbf{D}}_L$ is an increment in $\mathbf{D}_L$. Let $\dot{\mathbf{T}}$ and $\dot{\mathbf{E}}_L$ be increments in $\mathbf{T}$ and $\mathbf{E}_L$, respectively. Then, the incremental forms of the governing equations (4) and (7) are

$$\operatorname{Curl}\dot{\mathbf{E}}_L = \mathbf{0}, \quad \operatorname{Div}\dot{\mathbf{D}}_L = 0, \quad \operatorname{Div}\dot{\mathbf{T}} = \rho\dot{\mathbf{x}}_{,tt}. \tag{14}$$

When linearized in the increments, the incremental forms of the constitutive equations (8) become

$$\dot{\mathbf{T}} = \boldsymbol{\mathcal{A}}^*\dot{\mathbf{F}} + \boldsymbol{\Gamma}^*\dot{\mathbf{D}}_L - \dot{p}\mathbf{F}^{-1} + p\mathbf{F}^{-1}\dot{\mathbf{F}}\mathbf{F}^{-1}, \quad \dot{\mathbf{E}}_L = \boldsymbol{\Gamma}^{*T}\dot{\mathbf{F}} + \mathsf{K}^*\dot{\mathbf{D}}_L, \tag{15}$$

where $\dot{p}$ is the increment in p and $\boldsymbol{\mathcal{A}}^*$, $\boldsymbol{\Gamma}^*$ and K^* are, respectively, fourth-, third- and second-order tensors, which are referred to as electroelastic moduli tensors [2]. Respectively, they represent the elasticity tensor at fixed $\mathbf{D}_L$, the electroelastic coupling tensor, and the reciprocal of the dielectric tensor at fixed deformation.

In (Cartesian) component form, the equations in (15) are written

$$\dot{T}_{\alpha i} = \mathcal{A}_{\alpha i\beta j}^*\dot{F}_{j\beta} + \Gamma_{\alpha i|\beta}^*\dot{D}_{L\beta}, \quad \dot{E}_{L\alpha} = \Gamma_{\beta i|\alpha}^*\dot{F}_{i\beta} + \mathsf{K}_{\alpha\beta}^*\dot{D}_{L\beta}, \tag{16}$$

where the components of the moduli tensors are defined by

$$\mathcal{A}_{\alpha i\beta j}^* = \frac{\partial^2\Omega^*}{\partial F_{i\alpha}\partial F_{j\beta}}, \quad \Gamma_{\alpha i|\beta}^* = \frac{\partial^2\Omega^*}{\partial F_{i\alpha}\partial D_{l\beta}}, \quad \mathsf{K}_{\alpha\beta}^* = \frac{\partial^2\Omega^*}{\partial D_{l\alpha}\partial D_{l\beta}}, \tag{17}$$

with $\mathbf{\Gamma}^{*T}$ defined in component form by $(\mathbf{\Gamma}^{*T})_{\alpha|\beta i} = (\mathbf{\Gamma}^*)_{\beta i|\alpha}$ and $\boldsymbol{\mathcal{A}}^*$ and $\mathbf{K}^*$ having the symmetries $\mathcal{A}^*_{\alpha i \beta j} = \mathcal{A}^*_{\beta j \alpha i}$, $\mathsf{K}^*_{\alpha\beta} = \mathsf{K}^*_{\beta\alpha}$.

In order to refer quantities to the deformed configuration $\mathcal{B}$ rather than the original reference configuration $\mathcal{B}_r$, we use pushforward versions of $\dot{\mathbf{T}}$, $\dot{\mathbf{D}}_L$, $\dot{\mathbf{E}}_L$, denoted by $\dot{\mathbf{T}}_0$, $\dot{\mathbf{D}}_{L0}$, $\dot{\mathbf{E}}_{L0}$, respectively, and (for an incompressible material) defined by

$$\dot{\mathbf{T}}_0 = \mathbf{F}\dot{\mathbf{T}}, \quad \dot{\mathbf{D}}_{L0} = \mathbf{F}\dot{\mathbf{D}}_L, \quad \dot{\mathbf{E}}_{L0} = \mathbf{F}^{-T}\dot{\mathbf{E}}_L. \tag{18}$$

The equations in (14) can then be transformed into their Eulerian counterparts as

$$\mathrm{curl}\,\dot{\mathbf{E}}_{L0} = \mathbf{0}, \quad \mathrm{div}\,\dot{\mathbf{D}}_{L0} = 0, \quad \mathrm{div}\,\dot{\mathbf{T}}_0 = \rho\dot{\mathbf{u}}_{,tt}, \tag{19}$$

where $\mathbf{u}$ is the incremental displacement $\dot{\mathbf{x}}$ when regarded as function of $\mathbf{x}$ and t (instead of $\mathbf{X}$ and t), and $\mathrm{grad}\,\mathbf{u} = \dot{\mathbf{F}}\mathbf{F}^{-1}$, which is the pushforward of $\dot{\mathbf{F}}$. Henceforth, we use the notation $\mathbf{H} = \mathrm{grad}\,\mathbf{u}$. Equations (19) are coupled with the incremental incompressibility condition

$$\mathrm{tr}\,\mathbf{H} \equiv \mathrm{div}\,\mathbf{u} = 0. \tag{20}$$

The incremental constitutive equations in (15) can then be recast in the pushforward forms

$$\dot{\mathbf{T}}_0 = \boldsymbol{\mathcal{A}}^*_0\mathbf{H} + \mathbf{\Gamma}^*_0\dot{\mathbf{D}}_{L0} + p\mathbf{H} - \dot{p}\mathbf{I}, \quad \dot{\mathbf{E}}_{L0} = \mathbf{\Gamma}^{*T}_0\mathbf{H} + \mathbf{K}^*_0\dot{\mathbf{D}}_{L0}, \tag{21}$$

where the updated moduli tensors $\boldsymbol{\mathcal{A}}^*_0$, $\mathbf{\Gamma}^*_0$ and $\mathbf{K}^*_0$ are related to $\boldsymbol{\mathcal{A}}^*$, $\mathbf{\Gamma}^*$ and $\mathbf{K}^*$ in component form by

$$\mathcal{A}^*_{0piqj} = F_{p\alpha}F_{q\beta}\mathcal{A}^*_{\alpha i \beta j}, \quad \Gamma^*_{0pi|q} = F_{p\alpha}F^{-1}_{\beta q}\Gamma^*_{\alpha i|\beta}, \quad \mathsf{K}^*_{0ij} = F^{-1}_{\alpha i}F^{-1}_{\beta j}\mathsf{K}^*_{\alpha\beta}, \tag{22}$$

with the symmetries $\mathcal{A}^*_{0piqj} = \mathcal{A}^*_{0qjpi}$, $\Gamma^*_{0pi|q} = \Gamma^*_{0ip|q}$, $\mathsf{K}^*_{0ij} = \mathsf{K}^*_{0ji}$. A complete list of the components of $\boldsymbol{\mathcal{A}}^*_0$, $\mathbf{\Gamma}^*_0$ and $\mathbf{K}^*_0$ for a general isotropic Ω^* can be found in the text [9].

Equations (19)–(21) govern the incremental displacement $\mathbf{u}$ and the incremental field $\dot{\mathbf{D}}_{L0}$ in Eulerian form.

4. Incremental exterior fields and boundary conditions

Noting the distinction between * and *, let $\mathbf{D}^\star$ and $\mathbf{E}^\star$ be the electric displacement and electric field outside the body connected by $\mathbf{D}^\star = \varepsilon_0\mathbf{E}^\star$, where ε_0 is the permittivity of free space. The corresponding incremental fields $\dot{\mathbf{D}}^\star$ and $\dot{\mathbf{E}}^\star$ are related by

$$\dot{\mathbf{D}}^\star = \varepsilon_0\dot{\mathbf{E}}^\star \tag{23}$$

and satisfy the equations

$$\mathrm{curl}\,\dot{\mathbf{E}}^\star = \mathbf{0}, \quad \mathrm{div}\,\dot{\mathbf{D}}^\star = 0. \tag{24}$$

The associated Maxwell stress, denoted $\boldsymbol{\tau}^\star$, and its increment $\dot{\boldsymbol{\tau}}^\star$ are given by

$$\boldsymbol{\tau}^\star = \varepsilon_0\left[\mathbf{E}^\star \otimes \mathbf{E}^\star - \frac{1}{2}(\mathbf{E}^\star \cdot \mathbf{E}^\star)\mathbf{I}\right], \quad \dot{\boldsymbol{\tau}}^\star = \varepsilon_0[\dot{\mathbf{E}}^\star \otimes \mathbf{E}^\star + \mathbf{E}^\star \otimes \dot{\mathbf{E}}^\star - (\mathbf{E}^\star \cdot \dot{\mathbf{E}}^\star)\mathbf{I}], \tag{25}$$

and satisfy $\mathrm{div}\,\boldsymbol{\tau}^\star = \mathbf{0}$, $\mathrm{div}\,\dot{\boldsymbol{\tau}}^\star = \mathbf{0}$.

Let $\mathbf{n}$ be the unit outward normal vector to $\partial\mathcal{B}$ and $\mathrm{d}a$ be the associated area element. Then, the traction on the area element may be written as $\boldsymbol{\tau}\mathbf{n}\mathrm{d}a$. The appropriate traction boundary condition in Eulerian form is

$$\boldsymbol{\tau}\mathbf{n} = \mathbf{t}_a + \mathbf{t}^\star_e, \tag{26}$$

where $\mathbf{t}_a$ is the applied mechanical traction per unit area of $\partial\mathcal{B}$ and $\mathbf{t}^\star_e$ is the part of traction due to the Maxwell stress exterior to the body. The above boundary condition may be written in Lagrangian form as

$$\mathbf{T}^T\mathbf{N} = \mathbf{t}_A + \mathbf{t}^\star_E, \tag{27}$$

where $\mathbf{t}_A$ and $\mathbf{t}_E^\star$ are related to $\mathbf{t}_a$ and $\mathbf{t}_e^\star$ by $\mathbf{t}_A dA = \mathbf{t}_a da$ and $\mathbf{t}_E^\star dA = \mathbf{t}_e^\star da$, respectively. Here $\mathbf{N}$ is the unit outward normal vector to $\partial \mathcal{B}_r$ and dA is the associated area element.

By Nanson's formula $\mathbf{n}da = \mathbf{F}^{-T}\mathbf{N}dA$ for an incompressible material, the exterior Maxwell traction $\mathbf{t}_E^\star$ is written as $\mathbf{t}_E^\star = \boldsymbol{\tau}^\star \mathbf{F}^{-T}\mathbf{N}$ per unit reference area. Then, the above boundary condition becomes

$$\mathbf{T}^T\mathbf{N} = \mathbf{t}_A + \boldsymbol{\tau}^\star \mathbf{F}^{-T}\mathbf{N}. \tag{28}$$

On taking the increment of this equation, we obtain

$$\dot{\mathbf{T}}^T\mathbf{N} = \dot{\mathbf{t}}_A + \dot{\boldsymbol{\tau}}^\star \mathbf{F}^{-T}\mathbf{N} - \boldsymbol{\tau}^\star \mathbf{F}^{-T}\dot{\mathbf{F}}^T\mathbf{F}^{-T}\mathbf{N} \tag{29}$$

on $\partial \mathcal{B}_r$, and in updated (Eulerian) form

$$\dot{\mathbf{T}}_0^T\mathbf{N} = \dot{\mathbf{t}}_{A0} + \dot{\boldsymbol{\tau}}^\star \mathbf{n} - \boldsymbol{\tau}^\star \mathbf{H}^T\mathbf{n}, \tag{30}$$

on $\partial \mathcal{B}$.

The boundary conditions for the electric displacement and electric field in Eulerian form are

$$(\mathbf{D} - \mathbf{D}^\star) \cdot \mathbf{n} = 0, \quad (\mathbf{E} - \mathbf{E}^\star) \times \mathbf{n} = \mathbf{0}, \tag{31}$$

where each term is evaluated on $\partial \mathcal{B}$, it being assumed that there are no surface charges. In Lagrangian form, they become

$$(\mathbf{D}_L - \mathbf{F}^{-1}\mathbf{D}^\star) \cdot \mathbf{N} = 0, \quad (\mathbf{E}_L - \mathbf{F}^T\mathbf{E}^\star) \times \mathbf{N} = \mathbf{0}, \tag{32}$$

which apply on the boundary $\partial \mathcal{B}_r$. On taking the increments of these and then updating, we obtain

$$[\dot{\mathbf{D}}_{L0} - \dot{\mathbf{D}}^\star + \mathbf{H}\mathbf{D}^\star] \cdot \mathbf{n} = 0, \quad [\dot{\mathbf{E}}_{L0} - \dot{\mathbf{E}}^\star - \mathbf{H}^T\mathbf{E}^\star] \times \mathbf{n} = \mathbf{0}, \tag{33}$$

both of which hold on $\partial \mathcal{B}$.

5. Two-dimensional incremental motions

We now restrict attention to plane strain in the $(1, 2)$ plane with $D_3 = 0$ and also consider the incremental displacement components to have the forms

$$u_1 = u_1(x_1, x_2, t), \quad u_2 = u_2(x_1, x_2, t), \quad u_3 = 0, \tag{34}$$

while the incremental Lagrange multiplier is given by $\dot{p} = \dot{p}(x_1, x_2, t)$. Similarly, we take the components of the incremental electric displacement vector to be

$$\dot{D}_{L01} = \dot{D}_{L01}(x_1, x_2, t), \quad \dot{D}_{L02} = \dot{D}_{L02}(x_1, x_2, t), \quad \dot{D}_{L03} = 0. \tag{35}$$

In what follows, a subscript i following a comma indicates partial differentiation with respect to x_i, $i = 1, 2$.

In this specialization, the incremental incompressibility condition (20) and Eq. (19)$_2$ reduce to

$$u_{1,1} + u_{2,2} = 0, \quad \dot{D}_{L01,1} + \dot{D}_{L02,2} = 0, \tag{36}$$

from which we deduce the existence of functions $\psi = \psi(x_1, x_2, t)$ and $\varphi = \varphi(x_1, x_2, t)$ such that

$$u_1 = \psi_{,2}, \quad u_2 = -\psi_{,1}, \quad \dot{D}_{L01} = \varphi_{,2}, \quad \dot{D}_{L02} = -\varphi_{,1}. \tag{37}$$

The incremental equation of motion (19)$_3$ specializes to the two-component form as

$$\dot{T}_{011,1} + \dot{T}_{021,2} = \rho u_{1,tt}, \quad \dot{T}_{012,1} + \dot{T}_{022,2} = \rho u_{2,tt}, \tag{38}$$

and Eq. (19)$_1$ reduces to

$$\dot{E}_{L01,2} - \dot{E}_{L02,1} = 0. \tag{39}$$

The relevant components of the incremental stresses and electric field are obtained by specializing the incremental constitutive equations (21), yielding

$$\dot{T}_{011} = (\mathcal{A}^*_{01111} + p)u_{1,1} + \mathcal{A}^*_{01121}u_{1,2} + \mathcal{A}^*_{01112}u_{2,1} + \mathcal{A}^*_{01122}u_{2,2} + \Gamma^*_{011|1}\dot{D}_{L01} + \Gamma^*_{011|2}\dot{D}_{L02} - \dot{p},$$

$$\dot{T}_{012} = \mathcal{A}^*_{01211}u_{1,1} + (\mathcal{A}^*_{01221} + p)u_{1,2} + \mathcal{A}^*_{01212}u_{2,1} + \mathcal{A}^*_{01222}u_{2,2} + \Gamma^*_{012|1}\dot{D}_{L01} + \Gamma^*_{012|2}\dot{D}_{L02},$$

$$\dot{T}_{021} = \mathcal{A}^*_{02111}u_{1,1} + \mathcal{A}^*_{02121}u_{1,2} + (\mathcal{A}^*_{02112} + p)u_{2,1} + \mathcal{A}^*_{02122}u_{2,2} + \Gamma^*_{021|1}\dot{D}_{L01} + \Gamma^*_{021|2}\dot{D}_{L02},$$

$$\dot{T}_{022} = \mathcal{A}^*_{01122}u_{1,1} + \mathcal{A}^*_{02221}u_{1,2} + \mathcal{A}^*_{02212}u_{2,1} + (\mathcal{A}^*_{02222} + p)u_{2,2} + \Gamma^*_{022|1}\dot{D}_{L01} + \Gamma^*_{022|2}\dot{D}_{L02} - \dot{p},$$

$$(40)$$

and

$$\dot{E}_{L01} = \Gamma^*_{011|1}u_{1,1} + \Gamma^*_{012|1}(u_{1,2} + u_{2,1}) + \Gamma^*_{022|1}u_{2,2} + \mathsf{K}^*_{011}\dot{D}_{L01} + \mathsf{K}^*_{012}\dot{D}_{L02},$$

$$\dot{E}_{L02} = \Gamma^*_{011|2}u_{1,1} + \Gamma^*_{012|2}(u_{1,2} + u_{2,1}) + \Gamma^*_{022|2}u_{2,2} + \mathsf{K}^*_{012}\dot{D}_{L01} + \mathsf{K}^*_{022}\dot{D}_{L02}. \qquad (41)$$

5.1. Specialization of the underlying configuration

In this section, the preceding equations and the boundary conditions from Sect. 4 are specialized for the pure homogeneous deformation of an electroelastic half-space in the presence of an electric field normal to its boundary. The pure homogeneous plane strain is described with reference to rectangular Cartesian coordinates (X_1, X_2, X_3) in the undeformed configuration and (x_1, x_2, x_3) in the deformed configuration by

$$x_1 = \lambda X_1, \quad x_2 = \lambda^{-1}X_2, \quad x_3 = X_3, \qquad (42)$$

where λ is constant, and the half-space is taken to occupy the region $x_2 < 0$ in the deformed configuration, with boundary $x_2 = 0$. For this deformation, the deformation gradient $\mathbf{F}$ is diagonal with respect to the chosen (principal) axes of the deformation and the principal stretches are $\lambda_1 = \lambda$, $\lambda_2 = \lambda^{-1}$, $\lambda_3 = 1$. Then, the invariants I_1 and I_2 are obtained from Eq. (10) as

$$I_1 = I_2 = 1 + \lambda^2 + \lambda^{-2}. \qquad (43)$$

We take $\mathbf{D}$ to be aligned with the x_2 axis, so that $D_1 = D_3 = 0$ and D_2 is constant. The corresponding Lagrangian field has components $D_{L1} = D_{L3} = 0$ and $D_{L2} = \lambda D_2$, and the invariants I_4, I_5 and I_6 are obtained from Eq. (11) as

$$I_4 = D_{L2}^2, \quad I_5 = \lambda^{-2}D_{L2}^2, \quad I_5 = \lambda^{-4}D_{L2}^2. \qquad (44)$$

From (12) and (13), the only nonzero components of $\boldsymbol{\tau}$ and $\mathbf{E}$ are obtained as

$$\tau_{11} = 2\Omega^*_1\lambda^2 + 2\Omega^*_2(\lambda^2 + 1) - p, \qquad (45)$$

$$\tau_{22} = 2\Omega^*_1\lambda^{-2} + 2\Omega^*_2(1 + \lambda^{-2}) - p + 2\Omega^*_5\lambda^{-2}I_4 + 4\Omega^*_6\lambda^{-4}I_4, \qquad (46)$$

$$\tau_{33} = 2\Omega^*_1 + 2\Omega^*_2(\lambda^2 + \lambda^{-2}) - p, \qquad (47)$$

and

$$E_2 = 2(\lambda^2\Omega^*_4 + \Omega^*_5 + \lambda^{-2}\Omega^*_6)D_2. \qquad (48)$$

In this configuration, the components of the tensors $\mathcal{A}^*_0$, Γ^*_0 and K^*_0 are also reduced in number. In particular, the coefficients in Eqs. (40) and (41) are such that the components $\mathcal{A}^*_{0ijkl}$ with three indices 1 or three indices 2 vanish, $\Gamma^*_{011|1} = \Gamma^*_{022|1} = \Gamma_{011|2} = 0$, $\Gamma^*_{012|2} = \Gamma^*_{021|2} = 0$ and $\mathsf{K}^*_{012} = 0$ (see [9] for full details of the component expressions).

Equations (38) and (39) can then be arranged as two equations coupling ψ and φ, namely

$$a\psi_{,1111} + 2b\psi_{,1122} + c\psi_{,2222} + (e - d)\varphi_{,112} + d\varphi_{,222} = \rho(\psi_{,11tt} + \psi_{,22tt}), \qquad (49)$$

$$(e - d)\psi_{,112} + d\psi_{,222} + g\varphi_{,11} + f\varphi_{,22} = 0, \qquad (50)$$

within which the following notations have been introduced:

$$a = \mathcal{A}^*_{01212}, \quad 2b = \mathcal{A}^*_{01111} + \mathcal{A}^*_{02222} - 2\mathcal{A}^*_{01122} - 2\mathcal{A}^*_{01221}, \quad c = \mathcal{A}^*_{02121}, \qquad (51)$$

$$d = \Gamma^*_{012|1} = \Gamma^*_{021|1}, \quad e = \Gamma^*_{022|2}, \quad f = \mathsf{K}^*_{011}, \quad g = \mathsf{K}^*_{022}. \qquad (52)$$

Since the underlying electric displacement field has just a single component D_2 and $E_1 = E_3 = 0$ in the material, then, on applying the above boundary conditions on $x_2 = 0$, we have $D_2^\star = D_2$, $E_1^\star = E_3^\star = 0$, and from relation $\mathbf{D}^\star = \varepsilon_0 \mathbf{E}^\star$, it follows that $D_1^\star = D_3^\star = 0$ and $E_2^\star = \varepsilon_0^{-1} D_2$. The equations in (1) then ensure that outside the material the electric displacement field is uniform and related to the internal Lagrangian field via $D_2^\star = D_2 = \lambda^{-1} D_{L2}$. From Eq. (25), the nonzero components of the Maxwell stress $\boldsymbol{\tau}^\star$ are obtained as

$$\tau_{11}^\star = \tau_{33}^\star = -\tau_{22}^\star = -\frac{1}{2}\varepsilon_0^{-1} D_2^2. \tag{53}$$

In general, $\tau_{22} \neq \tau_{22}^\star$, so that an applied mechanical traction is required on $x_2 = 0$ in order to balance the difference $\tau_{22} - \tau_{22}^\star$.

Since the incremental fields are independent of x_3 in the considered specialization, we deduce the existence of a scalar function $\varphi^\star = \varphi^\star(x_1, x_2, t)$ such that

$$\dot{E}_1^\star = -\varphi_{,1}^\star, \quad \dot{E}_2^\star = -\varphi_{,2}^\star, \tag{54}$$

where $\varphi^\star$ satisfy Laplace's equation in $x_2 > 0$. The nonzero components of the incremental Maxwell stress tensor in (25) are then

$$\dot{\tau}_{11}^\star = \dot{\tau}_{33}^\star = -\dot{\tau}_{22}^\star = D_2 \varphi_{,2}^\star, \quad \dot{\tau}_{12}^\star = \dot{\tau}_{21}^\star = -D_2 \varphi_{,1}^\star. \tag{55}$$

In the present situation, we take the incremental mechanical traction on the boundary to vanish, so that the following two boundary conditions are obtained from (30):

$$\dot{T}_{021} + \tau_{11}^\star u_{2,1} - \dot{\tau}_{12}^\star = 0, \quad \dot{T}_{022} + \tau_{22}^\star u_{2,2} - \dot{\tau}_{22}^\star = 0 \quad \text{on } x_2 = 0. \tag{56}$$

The incremental electric boundary conditions (33) specialize as

$$\dot{E}_{L01} - \dot{E}_1^\star - E_2^\star u_{2,1} = 0, \quad \dot{D}_{L02} - \dot{D}_2^\star + D_2^\star u_{2,2} = 0 \quad \text{on } x_2 = 0. \tag{57}$$

Following [2], we assume that there is no applied mechanical traction on $x_2 = 0$ in the underlying configuration, so that $\tau_{22} = \tau_{22}^\star = \varepsilon_0^{-1} D_2^2/2$. In terms of the scalar functions ψ, φ and $\varphi^\star$, the incremental boundary conditions (56) and (57) then become

$$(\varepsilon_0^{-1} D_2^2 - c)\psi_{,11} + c\psi_{,22} + d\varphi_{,2} + D_2\varphi_{,1}^\star = 0 \quad \text{on } x_2 = 0, \tag{58}$$

$$(2b + c)\psi_{,112} + c\psi_{,222} + e\varphi_{,11} + d\varphi_{,22} - D_2\varphi_{,12}^\star - \rho\psi_{,2tt} = 0 \quad \text{on } x_2 = 0, \tag{59}$$

$$(\varepsilon_0^{-1} D_2 - d)\psi_{,11} + d\psi_{,22} + f\varphi_{,2} + \varphi_{,1}^\star = 0 \quad \text{on } x_2 = 0, \tag{60}$$

$$D_2\psi_{,12} + \varphi_{,1} - \varepsilon_0\varphi_{,2}^\star = 0 \quad \text{on } x_2 = 0. \tag{61}$$

Equation (59) is obtained by differentiating $(56)_2$ with respect to x_1 and then making use made of the expression for $\dot{p}_{,1}$ from $(38)_1$. Equations (58)–(61) are equivalent to those obtained in [2] for the corresponding situation.

On elimination of $\varphi_{,1}^\star$ from Eqs. (58) and (60) and elimination of $\varphi_{,12}^\star$ from Eqs. (59) and (61) after differentiating the latter with respect to x_1, the boundary conditions required for Eqs. (49) and (50) in terms of the scalar functions ψ and φ are

$$(D_2 d - c)(\psi_{,11} - \psi_{,22}) + (d - D_2 f)\varphi_{,2} = 0 \quad \text{on } x_2 = 0, \tag{62}$$

$$(2b + c - \varepsilon_0^{-1} D_2^2)\psi_{,112} + c\psi_{,222} + (e - \varepsilon_0^{-1} D_2)\varphi_{,11} + d\varphi_{,22} - \rho\psi_{,2tt} = 0 \quad \text{on } x_2 = 0. \tag{63}$$

The exterior field can now be ignored and we are left with the two Eqs. (49) and (50) and the associated boundary conditions (62) and (63) involving ψ and φ.

5.1.1. A simple model energy function. The energy function Ω^* for a simple prototype model of nonlinear electroelasticity, introduced in [2], is given by

$$\Omega^* = \frac{1}{2}\mu(I_1 - 3) + \varepsilon_0^{-1}(\alpha I_4 + \beta I_5), \tag{64}$$

where the constant $\mu > 0$ is the shear modulus of a neo-Hookean material in the configuration $\mathcal{B}_r$ (in the absence of an electric field) and $\alpha \geq 0$ and $\beta > 0$ are constant electroelastic parameters. Note that if $\alpha = \beta = 0$ the problem is purely elastic and has been discussed in detail in [3].

For this energy function, Eq. (48) reduces to

$$E_2 = 2\varepsilon_0^{-1}(\alpha\lambda^2 + \beta)D_2, \tag{65}$$

so that $\varepsilon \equiv \varepsilon_0/2(\alpha\lambda^2 + \beta)$ has the interpretation as the material permittivity, which for $\alpha \neq 0$ is deformation dependent. In the undeformed configuration, the relative permittivity $\varepsilon/\varepsilon_0 > 1$, so that the restriction $\alpha + \beta < 1/2$ applies. The material parameters (51) and (52) reduce to

$$a = \mu\lambda^2, \quad c = \mu(\lambda^{-2} + 2\beta\hat{D}_2^2), \quad 2b = a + c, \tag{66}$$
$$e - d = d = 2\varepsilon_0^{-1}\beta D_2, \quad f = 2\varepsilon_0^{-1}(\alpha\lambda^{-2} + \beta), \quad g = 2\varepsilon_0^{-1}(\alpha\lambda^2 + \beta), \tag{67}$$

where $\hat{D}_2$ is a dimensionless measure of D_2 defined by

$$\hat{D}_2 = D_2/\sqrt{\mu\varepsilon_0}. \tag{68}$$

In view of the relations $2b = a + c$ and $e = 2d$, Eqs. (49) and (50) and boundary conditions (62) and (63) specialize accordingly, and henceforth, we adopt this specialization.

6. Plane waves

We now consider plane waves propagating in an incompressible finitely deformed electroactive material. We assume that ψ and φ have the forms

$$\psi = \psi_0(n_1 x_1 + n_2 x_2 - vt), \quad \varphi = \varphi_0(n_1 x_1 + n_2 x_2 - vt), \tag{69}$$

where v is the wave speed, t is time, ψ_0 and φ_0 are functions of the indicated argument and n_1, n_2 with $n_3 = 0$ are components of the direction of propagation $\mathbf{n}$, with $(n_1, n_2) = (\cos\theta, \sin\theta)$, so that

$$n_1^2 + n_2^2 = 1. \tag{70}$$

On substituting (69) into Eqs. (49) and (50) with the indicated specialization, we obtain

$$(an_1^2 + cn_2^2 - \rho v^2)\psi_0'''' + dn_2\varphi_0''' = 0, \tag{71}$$
$$dn_2\psi_0''' + (gn_1^2 + fn_2^2)\varphi_0'' = 0, \tag{72}$$

where a prime signifies differentiation with respect to the argument.

After differentiating (72), we obtain a linear system for ψ_0'''' and φ_0''', which has a non-trivial solution if the determinant of coefficients vanishes. Following [2], this results in the following expression for the wave speed v:

$$\rho v^2 = an_1^2 + cn_2^2 - \frac{d^2 n_2^2}{gn_1^2 + fn_2^2}. \tag{73}$$

This equation determines the wave speed for any given direction of propagation in the (x_1, x_2) plane provided $\rho v^2 > 0$. It also determines possible directions in which waves may propagate for a given speed, material constants, and deformation. We now consider two cases.

Case (i): $\lambda = 1$. For the undeformed configuration, we have $a = \mu, c - a = dD_2, d = 2\varepsilon_0^{-1}\beta D_2, f = g = 2\varepsilon_0^{-1}(\alpha + \beta)$ and Eq. (73) is written in the form

$$\cos^2 \theta = \frac{cf - d^2 - \rho v^2 f}{cf - d^2 - af}. \tag{74}$$

For this equation to yield a real value of $\cos \theta$, we must have

$$1 \le \frac{\rho v^2}{\mu} \le 1 + \frac{2\alpha\beta\hat{D}_2^2}{\alpha + \beta}. \tag{75}$$

The two limits correspond to $\theta = 0$ and $\theta = \pi/2$, and we note that

$$\frac{\rho v^2}{\mu} = 1 + \frac{2\alpha\beta\hat{D}_2^2 n_2^2}{\alpha + \beta}. \tag{76}$$

Thus, $\rho v^2 = \mu$ if either $\alpha = 0$, $\beta = 0$ or $\hat{D}_2 = 0$.

Case (ii): $\lambda \neq 1$. For a given wave speed v, (73) may be written as a quadratic equation for n_1^2:

$$(c - a)(f - g)n_1^4 - [(c - a)f + (f - g)(c - \rho v^2) - d^2]n_1^2 + f(c - \rho v^2) - d^2 = 0. \tag{77}$$

This determines possible angles of propagation for a given wave speed, material properties, and deformation.

7. Wave reflection from the half-space boundary

We now consider plane waves of the form given by (69) incident on the boundary $x_2 = 0$ from within the half-space $x_2 < 0$. The incremental boundary conditions on $x_2 = 0$ are given by Eqs. (62) and (63). Let $(n_1, n_2) = (\cos \theta, \sin \theta)$ be the direction of propagation of an incident wave and v its speed.

The material properties and the state of deformation determine whether there are two reflected waves, or just one reflected wave together with a surface wave. The general solutions for ψ and φ consisting of the incident and (possibly) two reflected waves are assumed in the forms

$$\psi = Ae^{ik(n_1 x_1 + n_2 x_2 - vt)} + ARe^{ik(n_1 x_1 - n_2 x_2 - vt)} + AR'e^{ik'(n_1' x_1 - n_2' x_2 - v't)}, \tag{78}$$

$$\varphi = \xi_0 Ae^{ik(n_1 x_1 + n_2 x_2 - vt)} + \xi_1 ARe^{ik(n_1 x_1 - n_2 x_2 - t)} + \xi_1' AR'e^{ik'(n_1' x_1 - n_2' x_2 - v't)}, \tag{79}$$

where A is a constant, k and k' are the wave numbers, and v and v' the wave speeds. The coupling coefficients ξ_0, ξ_1 and ξ_1' are obtained from Eqs. (49) and (50) as

$$\xi_1 = -\xi_0 = \frac{ik(an_1^2 + cn_2^2 - \rho v^2)}{n_2 d} = \frac{ikdn_2}{gn_1^2 + fn_2^2}, \tag{80}$$

$$\xi_1' = \frac{ik'(an_1'^2 + cn_2'^2 - \rho v'^2)}{n_2' d} = \frac{ik'dn_2'}{gn_1'^2 + fn_2'^2}, \tag{81}$$

and R and R' are reflection coefficients. The speed of the first reflected wave is equal to the speed of the incident wave. Assuming that the first and second reflected waves are reflected at angles θ and θ' to the boundary, we have $n_1' = \cos \theta', n_2' = \sin \theta'$. The incident and reflected waves must have the same frequency, which requires

$$kv = k'v', \tag{82}$$

and the boundary conditions (62) and (63) require that $kn_1 = k'n_1'$. Hence

$$v'n_1 = vn_1', \tag{83}$$

which is a Snell's law for the case of two reflected waves. Note that for $g = f$, which is only possible for $\lambda = 1$ or $\alpha = 0$, Eq. (80) gives

$$\xi_0 = -\frac{\mathrm{i}kdn_2}{f} = -\frac{\mathrm{i}k\beta D_2 n_2}{\alpha\lambda^{-2} + \beta}. \tag{84}$$

7.1. Case (i) $\lambda = 1$

For two reflected waves, we have from (73), since $g = f$ when $\lambda = 1$,

$$\rho v^2 = f^{-1}[d^2 - (c - a)f]n_1^2 + f^{-1}(cf - d^2), \quad \rho v'^2 = f^{-1}[d^2 - (c - a)f]n_1'^2 + f^{-1}(cf - d^2). \tag{85}$$

Using Eq. (83) and eliminating v and v' from these two expressions, we obtain $n_1' = \pm n_1$. Thus, the two reflected waves coincide and there is only one reflected wave, and it is therefore necessary to consider a surface wave instead of a second reflected wave, as is done below.

7.2. Case (ii) $\lambda \neq 1$

Consider an incident wave with speed v given by (73), i.e.,

$$\rho v^2 = an_1^2 + cn_2^2 - \frac{d^2 n_2^2}{gn_1^2 + fn_2^2}, \tag{86}$$

and a reflected with speed v' given by

$$\rho v'^2 = an_1'^2 + cn_2'^2 - \frac{d^2 n_2'^2}{gn_1'^2 + fn_2'^2}. \tag{87}$$

Using Eq. (83) and eliminating v and v' between (86) and (87), we obtain *either* $n_1'^2 = n_1^2$ *or*

$$(g - f)[c(g - f) + d^2]n_1^2 n_1'^2 + (g - f)(cf - d^2)(n_1^2 + n_1'^2) + (cf - d^2)f = 0. \tag{88}$$

Noting that $cf - d^2 = 2\varepsilon_0^{-1}\lambda^{-2}[\mu(\alpha\lambda^{-2} + \beta) + 2\varepsilon_0^{-1}\alpha\beta D_2^2]$ is positive, it is straightforward to show that $n_1'^2 < 0$ when $g > f$, i.e., $\lambda > 1$, and $n_1'^2 > 0$ when $g < f$, i.e., $\lambda < 1$. While it is in principle possible that there could be two distinct reflected waves, with the second angle θ' ($n_1' = \cos\theta'$) satisfying (88), by forming an explicit expression for $n_1'^2$, which must satisfy $n_1'^2 \leq 1$, we find that this condition requires that $n_1^2 \geq (cf - d^2)/c(f - g)$, but for this also to be less that 1, we must have $cg - d^2 \equiv 2\mu\varepsilon_0^{-1}(\alpha + \beta\lambda^{-2} + 2\alpha\beta\lambda^2\hat{D}_2^2) \leq 0$, which cannot hold since $\alpha \geq 0$ and $\beta > 0$. Thus, in this case there can again be only one reflected wave, and the angle of reflection equals the angle of incidence.

We note that in the purely elastic context [3] the case in which the constitutive restriction $2b = a + c$ given in (66) holds also leads to just a single reflected wave, while if $2b \neq a + c$ two distinct reflected waves are possible. This will also be the case here if we choose a more general form of energy function, but this is not considered since our main purpose is to examine the basic influence of an electric field on the plane wave characteristics, their reflection at a half-space boundary and the generation of surface waves.

7.3. Surface waves

As only one reflected wave is possible, we now consider surface waves generated by a plane wave impinging on the boundary, and replace $n_1 x_1 + n_2 x_2 - vt$ in (69) by $x_1 - \mathrm{i}sx_2 - v't$. Then, a general solution consisting of an incident wave, a reflected wave and a surface wave is assumed in the form

$$\psi = A\mathrm{e}^{\mathrm{i}k(n_1 x_1 + n_2 x_2 - vt)} + AR\mathrm{e}^{\mathrm{i}k(n_1 x_1 - n_2 x_2 - vt)} + AR'\mathrm{e}^{\mathrm{i}k'(x_1 - \mathrm{i}sx_2 - v't)}, \tag{89}$$

$$\varphi = \xi_0 A\mathrm{e}^{\mathrm{i}k(n_1 x_1 + n_2 x_2 - vt)} + \xi_1 AR\mathrm{e}^{\mathrm{i}k(n_1 x_1 - n_2 x_2 - vt)} + \xi_1^* AR'\mathrm{e}^{\mathrm{i}k'(x_1 - \mathrm{i}sx_2 - v't)}, \tag{90}$$

and substituting into Eqs. (49) and (50), we obtain *either* $s^2 = 1$ *or* the counterpart of (73), which is

$$\rho v'^2 = a - cs^2 + \frac{d^2 s^2 (1 - s^2)}{g - fs^2}. \tag{91}$$

In the latter term, we have used the expression for ξ_1^* obtained from Eq. (50), which gives

$$\xi_1^*(g - fs^2) = -dk's(1 - s^2), \tag{92}$$

while $\xi_1 = -\xi_0$ is given by (80). In the special case, when $s^2 = 1$, Eq. (49) is satisfied automatically, while in the limit $s \to 1$ (92) gives

$$\xi_1^* = -\frac{k'd}{f} = -\frac{k'\beta D_2}{\alpha\lambda^{-2} + \beta}. \tag{93}$$

We require $s > 0$ for the surface wave terms in (89) and (90) to decay as $x_2 \to -\infty$. With Snell's law now in the form

$$kn_1 = k', \quad v'n_1 = v, \tag{94}$$

we obtain the counterpart of (88) for this case in the factorized form

$$(n_2^2 + s^2 n_1^2)\{(gn_1^2 + fn_2^2)(cf - d^2)s^2 - g[c(gn_1^2 + fn_2^2) - d^2]\} = 0. \tag{95}$$

The first factor recovers a reflected wave with angle of reflection equal to the angle of incidence, while for a surface wave ($s > 0$) the second factor yields

$$s = \sqrt{\frac{g[c(gn_1^2 + fn_2^2) - d^2]}{(gn_1^2 + fn_2^2)(cf - d^2)}}, \tag{96}$$

within which, for the values of the parameters given in (66) and (67), both numerator and denominator are positive for any angle of incidence.

At this point, it should be emphasized that the expression for v' given by (91) is not valid for $s = 1$ since consideration of (91) in conjunction with $v = v'n_1$ and (86) in the limit $s \to 1$ leads to $cf - d^2 = 0$, but for the considered model $cf - d^2 > 0$ when $\beta > 0$. It is thus important to distinguish between the cases $s = 1$ and $s \neq 1$ in the following. We first consider the case $s \neq 1$.

Substituting (89) and (90) into the boundary conditions (62) and (63), we obtain

$$\left[n_1^2 - n_2^2 - \frac{2\alpha\beta\hat{D}_2^2 n_2^2}{\alpha(\lambda^2 n_1^2 + \lambda^{-2} n_2^2) + \beta}\right](1 + R) + \left[1 + s^2 + \frac{2\alpha\beta\hat{D}_2^2 s^2(1 - s^2)}{\alpha(\lambda^2 - \lambda^{-2}s^2) + \beta(1 - s^2)}\right]R'n_1^2 = 0 \tag{97}$$

and, after use of (73) and (91),

$$\left[2\lambda^{-2} + (4\beta - 1)\hat{D}_2^2 - \frac{\beta(4\beta - 1)\hat{D}_2^2}{\alpha(\lambda^2 n_1^2 + \lambda^{-2} n_2^2) + \beta}\right](1 - R)n_1^2 n_2$$

$$-\mathrm{i}s\left[2\lambda^{-2} + (4\beta - 1)\hat{D}_2^2 - \frac{\beta(4\beta - 1)\hat{D}_2^2(1 - s^2)}{\alpha(\lambda^2 - \lambda^{-2}s^2) + \beta(1 - s^2)}\right]R'n_1^3 = 0. \tag{98}$$

Note that in respect of the coefficients of R' in (97) and (98), for $s \neq 1$ (and hence $f \neq g$), use of (96) shows that

$$2\varepsilon_0^{-1}[\alpha(\lambda^2 - \lambda^{-2}s^2) + \beta(1 - s^2)] = \frac{g(f - g)d^2 n_1^2}{(gn_1^2 + fn_2^2)(cf - d^2)}, \tag{99}$$

and the factor n_1^2 cancels with an n_1^2 in each of the terms that include the denominator $\alpha(\lambda^2 - \lambda^{-2}s^2) + \beta(1 - s^2)$.

From (97) and (98), we obtain the following values of R and R':

$$R = \frac{A_s B_n + A_n B_s}{A_s B_n - A_n B_s}, \quad R' = -\frac{2A_n B_n}{A_s B_n - A_n B_s}, \tag{100}$$

where

$$A_n = n_1^2 - n_2^2 - \frac{2\alpha\beta\hat{D}_2^2 n_2^2}{\alpha(\lambda^2 n_1^2 + \lambda^{-2} n_2^2) + \beta}, \tag{101}$$

$$A_s = (1+s^2)n_1^2 + \frac{\alpha[c(gn_1^2 + fn_2^2) - d^2][c(gn_1^2 + fn_2^2) - d^2 n_2^2]}{\mu\beta(gn_1^2 + fn_2^2)(cf - d^2)}, \tag{102}$$

$$B_n = n_1^2 n_2 \left[2\lambda^{-2} + (4\beta - 1)\hat{D}_2^2 - \frac{\beta(4\beta - 1)\hat{D}_2^2}{\alpha(\lambda^2 n_1^2 + \lambda^{-2} n_2^2) + \beta} \right], \tag{103}$$

$$B_s = -\mathrm{i}sn_1^3[2\lambda^{-2} + (4\beta - 1)\hat{D}_2^2] + \frac{\mathrm{i}sn_1(4\beta - 1)[c(gn_1^2 + fn_2^2) - d^2 n_2^2]}{2\mu\beta g}, \tag{104}$$

within which the expression (96) has been used.

It follows, in particular, that $|R| = 1$. Note that $R' = 0$, i.e., no surface wave is generated and there is only a reflected wave, if either $A_n = 0$ or $B_n = 0$, which is possible for a range of combinations of θ, α, β, λ and $\hat{D}_2$ and then $R = 1$ and $R = -1$, respectively. Note also that A_s and B_s reduce to A_n and B_n, respectively, when $s = \mathrm{i}n_2/n_1$, which corresponds to a reflected wave equivalent to that associated with R.

We now turn to the case $s = 1$. From Eq. (50) it follows, with $\xi_1^* \neq 0$, that $f = g$. The latter can only hold for $\alpha = 0$ or $\lambda = 1$. By following the procedure above but by using the expression (86) with $v = v'n_1$ instead of (91), we obtain, after multiplying by factors λ^2,

$$A_n = n_1^2 - n_2^2 - \frac{2\alpha\beta\lambda^2\hat{D}_2^2 n_2^2}{\alpha + \beta\lambda^2}, \quad A_s = 2n_1^2\left(1 + \frac{\alpha\beta\lambda^2\hat{D}_2^2}{\alpha + \beta\lambda^2}\right),$$

$$B_n = n_1^2 n_2 \left[2 + \frac{\alpha(4\beta - 1)\lambda^2\hat{D}_2^2}{\alpha + \beta\lambda^2}\right], \quad B_s = -\mathrm{i}n_1\left[\left(1 + \frac{2\alpha\beta\lambda^2\hat{D}_2^2}{\alpha + \beta\lambda^2}\right)(n_1^2 - n_2^2) - \frac{\alpha\lambda^2\hat{D}_2^2 n_1^2}{\alpha + \beta\lambda^2}\right]. \tag{105}$$

These expressions apply for either $\lambda = 1$ or $\alpha = 0$ with λ not necessarily equal to 1. In the latter case, R and R' are independent of λ. Note that if either $\alpha = 0$ or $\hat{D}_2 = 0$, this gives the result for the purely elastic case provided in [3] in the absence of normal stress.

The special case $\beta = 1/4$ deserves particular attention. If $\beta \neq 1/4$ or $\beta = 1/4$ and $\lambda = 1$ then $R \to -1$ and $R' \to 0$ as $n_1 \to 0$, but if $\beta = 1/4$ and $\lambda \neq 1$ then $R \to 1$ and $R' \to \lambda^2/2\alpha$ as $n_1 \to 0$. This is exemplified in the numerical results presented in the following section.
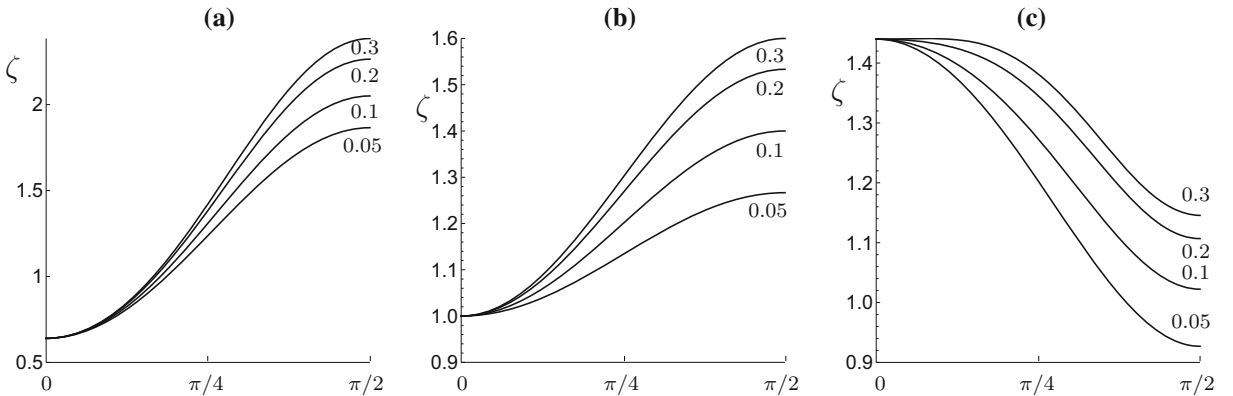

FIG. 1. Plots of the squared dimensionless wave speed $\zeta = \rho v^2/\mu$ against the angle of incidence $\theta \in [0, \pi/2]$ for $\alpha = 0.1$, $\beta = 0.05, 0.1, 0.2, 0.3$ and $\hat{D}_2 = 2$: **a** $\lambda = 0.8$; **b** $\lambda = 1$; **c** $\lambda = 1.2$
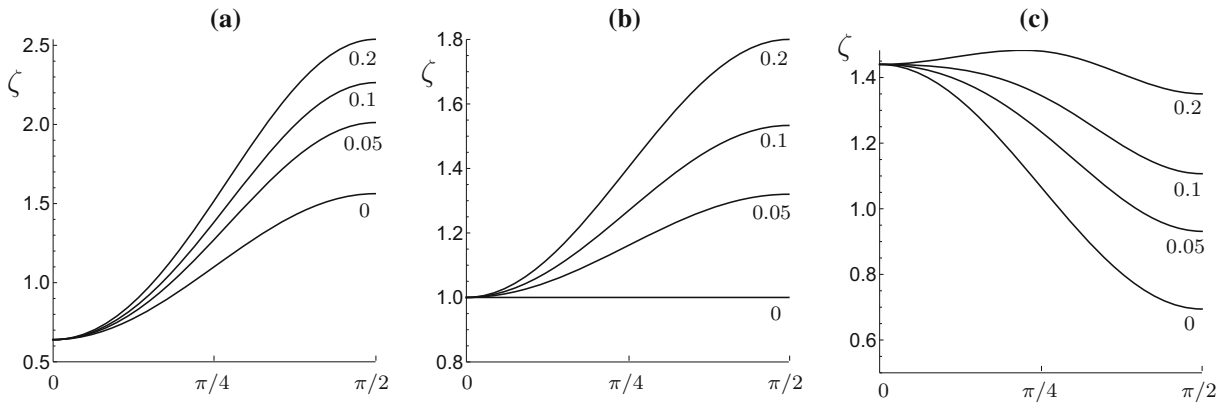
FIG. 2. Plots of the squared dimensionless wave speed $\zeta = \rho v^2/\mu$ against the angle of incidence $\theta \in [0, \pi/2]$ for $\beta = 0.2$, $\alpha = 0, 0.05, 0.1, 0.2$ and $\hat{D}_2 = 2$: **a** $\lambda = 0.8$; **b** $\lambda = 1$; **c** $\lambda = 1.2$
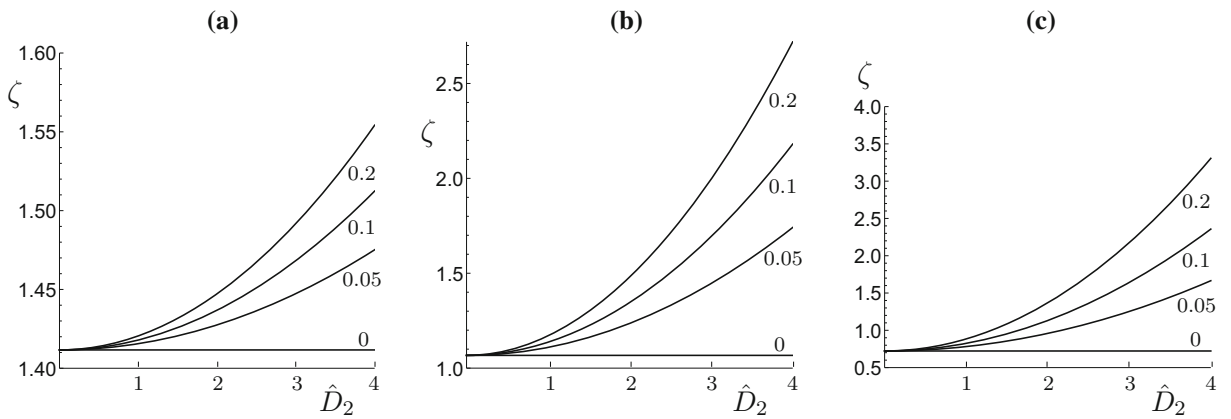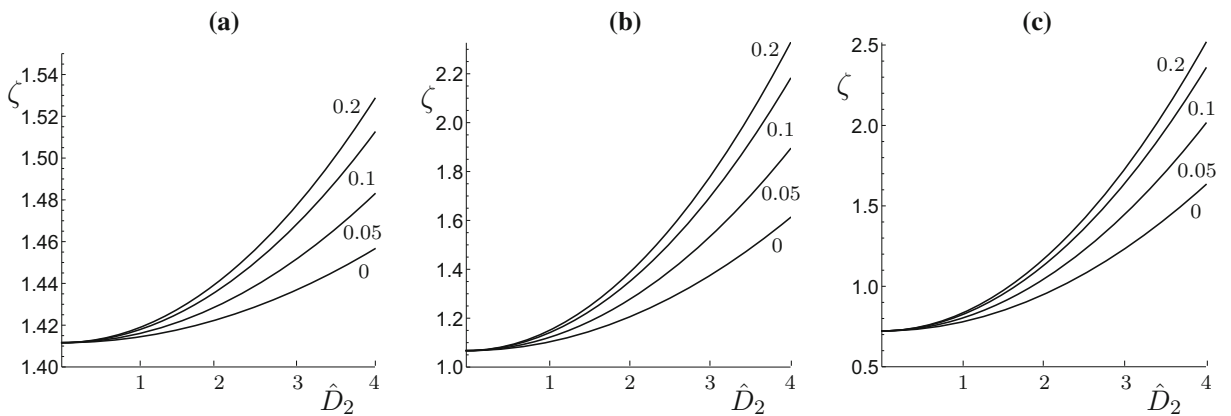

FIG. 3. Plots of the squared dimensionless wave speed $\zeta = \rho v^2/\mu$ against $\hat{D}_2 \in [0.4]$ for $\beta = 0.2$, $\alpha = 0, 0.05, 0.1, 0.2$ and $\lambda = 1.2$: **a** $\theta = \pi/16$; **b** $\theta = \pi/4$; **c** $\theta = 7\pi/16$

FIG. 4. Plots of the squared dimensionless wave speed $\zeta = \rho v^2/\mu$ against $\hat{D}_2 \in [0.4]$ for $\alpha = 0.1$, $\beta = 0.05, 0.1, 0.2, 0.3$ and $\lambda = 1.2$: **a** $\theta = \pi/16$; **b** $\theta = \pi/4$; **c** $\theta = 7\pi/16$
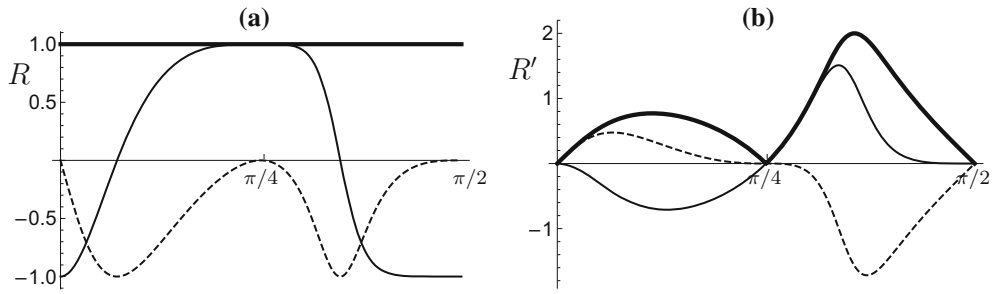
FIG. 5. Plots of the real and imaginary parts of R and R' (continuous and dashed curves, respectively) and $|R|$, $|R'|$ (thick continuous curves) for $\lambda = 1$ with $\alpha = 0$ (or $\hat{D}_2 = 0$): **a** R; **b** R'
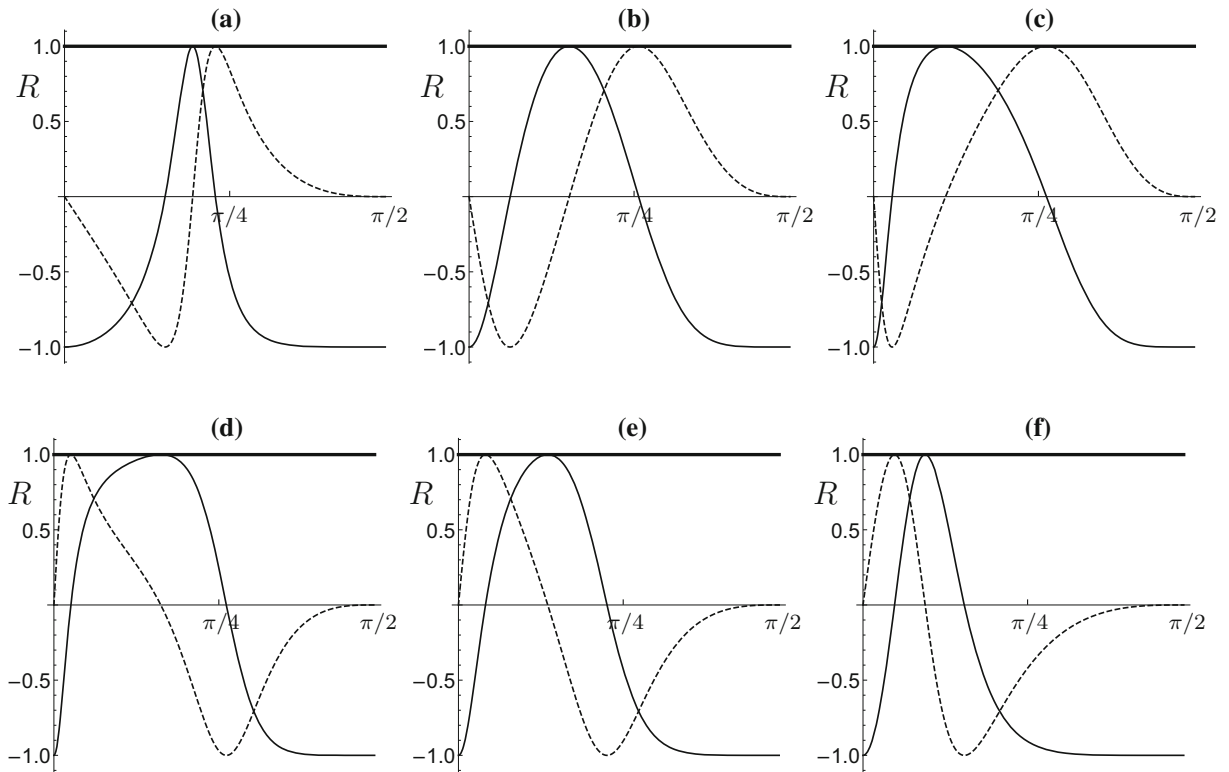
FIG. 6. Plots of $\mathrm{Re}(R)$, continuous curves, $\mathrm{Im}(R)$, dashed curves, and $|R| = 1$, versus $\theta \in [0, \pi/2]$ for $\lambda = 1$ with $\alpha = 0.1$: **a** $\beta = 0.1$, $\hat{D}_2 = 3$; **b** $\beta = 0.1$, $\hat{D}_2 = 5$; **c** $\beta = 0.1$, $\hat{D}_2 = 8$; **d** $\beta = 0.25$, $\hat{D}_2 = 3$; **e** $\beta = 0.25$, $\hat{D}_2 = 5$; **f** $\beta = 0.25$, $\hat{D}_2 = 8$

8. Results

From Eq. (73), the dimensionless form of the squared wave speed $\zeta = \rho c^2/\mu$ of plane waves is computed as a function of angle of propagation. This is plotted against the angle of propagation θ for different combinations of the values of coupling parameters α and β when the values of the stretch λ and dimensionless constant $\hat{D}_2$ are prescribed.
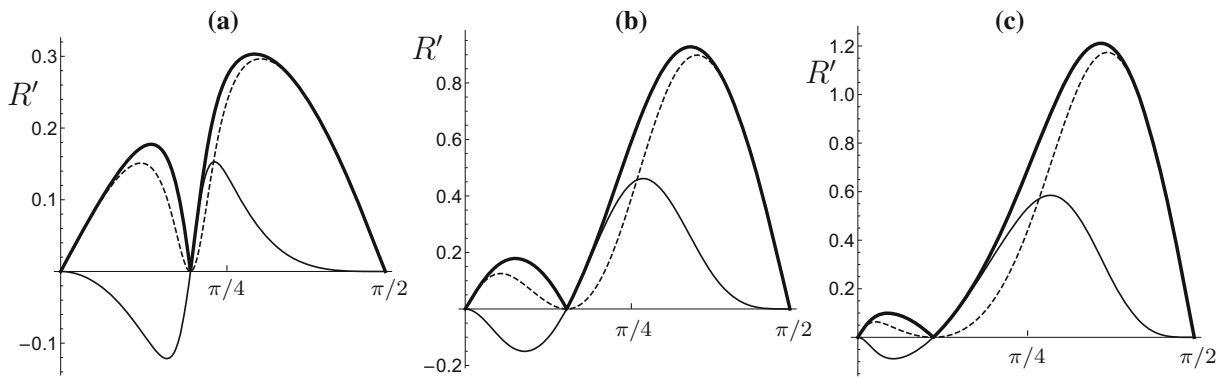
FIG. 7. Plots of Re(R'), continuous curves, Im(R'), dashed curves, and $|R'|$, thick continuous curves, versus θ for $\lambda = 1$, $\alpha = \beta = 0.1$: **a** $\hat{D}_2 = 3$; **b** $\hat{D}_2 = 5$; **c** $\hat{D}_2 = 8$
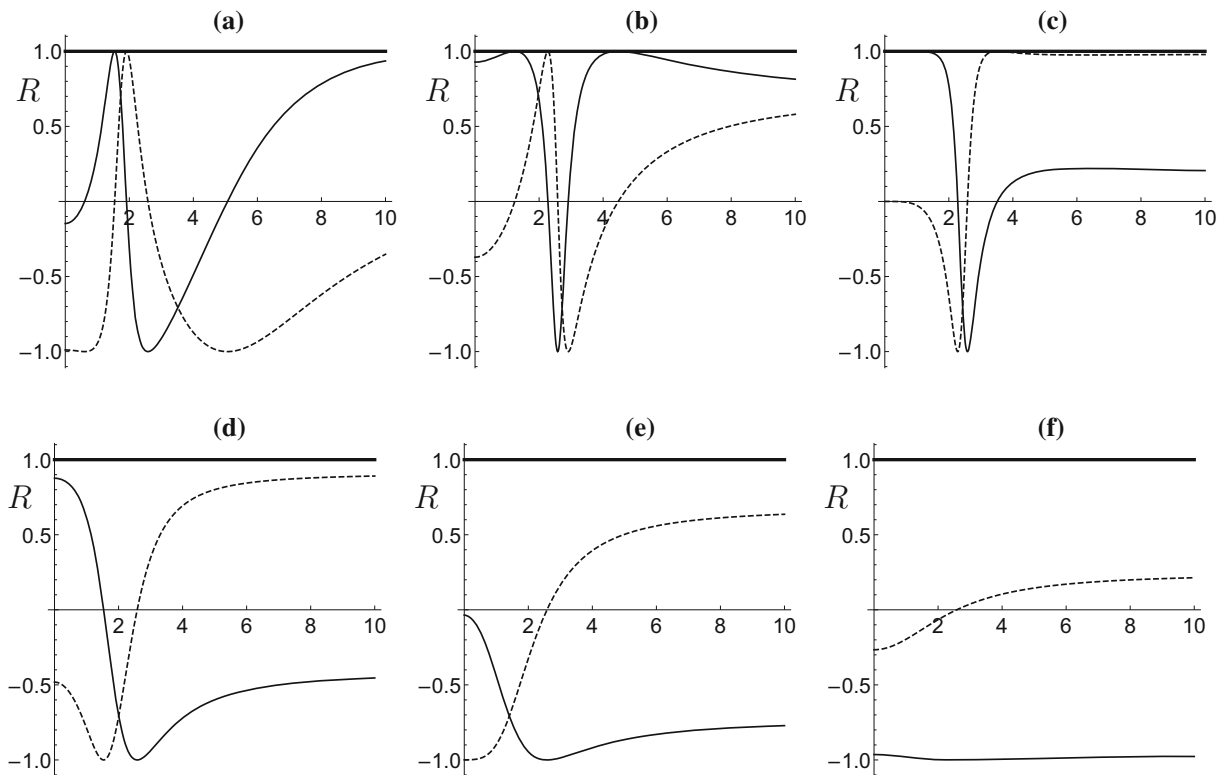

FIG. 8. Plots of Re(R), continuous curves, Im(R), dashed curves, and $|R| = 1$, versus $d \in [0, 10]$ for $\lambda = 1$, $\alpha = \beta = 0.1$ for different angles of incidence: **a** $\theta = \pi/16$; **b** $\theta = \pi/6$; **c** $\theta = \pi/4$; **d** $\theta = 5\pi/16$; **e** $\theta = 5.6\pi/16$; **f** $\theta = 6.5\pi/16$

In Fig. 1a–c, for $\lambda = 0.8$, $\lambda = 1$ and $\lambda = 1.2$, respectively, ζ is shown as a function of the angle of incidence θ for the representative values $\alpha = 0.1$ and $\hat{D}_2 = 2$ and for the four different values, 0.05, 0.1, 0.2 and 0.3, of β in each case. Note that for the relative permittivity of the material to be greater than 1 in the reference configuration we must have $\alpha + \beta < 1/2$ and the values of α and β have been chosen

(a)

(b)

(c)

(d)

(e)

(f)
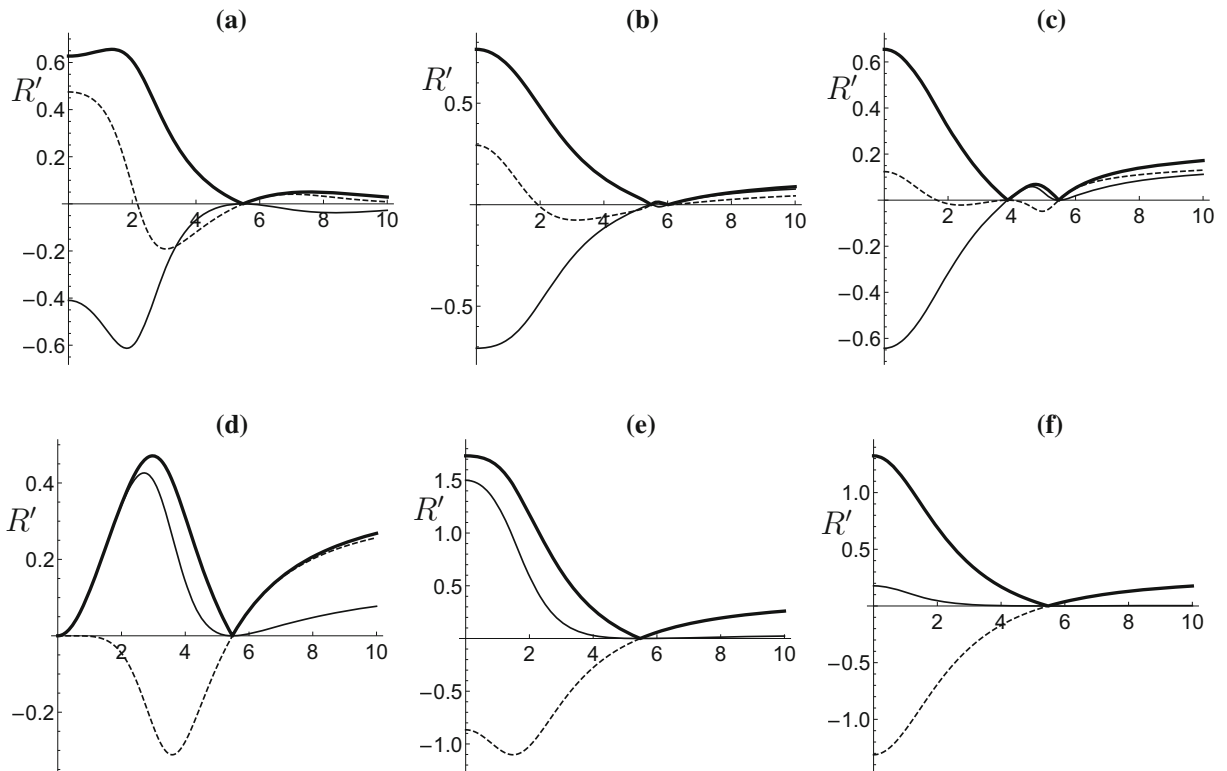
FIG. 9. Plots of $\mathrm{Re}(R')$, continuous curves, $\mathrm{Im}(R')$, dashed curves, and $|R'|$, thick continuous curves, versus $\hat{D}_2 \in [0, 10]$ for $\lambda = 1$, $\alpha = 0.1$, $\beta = 0.2$ for different angles of incidence: **a** $\theta = \pi/16$; **b** $\theta = \pi/8$; **c** $\theta = \pi/6$; **d** $\theta = \pi/4$; **e** $\theta = \pi/3$; **f** $\theta = 13\pi/32$

to respect this inequality. It can be seen that for $\lambda = 0.8$ and 1 the wave speed increases with the angle of propagation, while for $\lambda = 1.2$ it decreases. For each angle (except the grazing angle $\theta = 0$) and each value of λ the wave speed increases with increases in the value of β. The effect of the coupling parameter β increases with an increase in θ and it is maximum for normal incidence ($\theta = \pi/2$). The effect of the value of λ on the wave speed can be seen by comparing the curves in the three figures for specific values of β.

In Fig. 2a–c, corresponding results are illustrated again for $\lambda = 0.8$, $\lambda = 1$ and $\lambda = 1.2$ and $\hat{D}_2 = 2$, but now for the fixed value $\beta = 0.2$ and with our different values, 0, 0.05, 0.1, and 0.2 of α. For $\lambda = 0.8$ and 1 the plots have a similar character to those shown in Fig. 1a, b except that for $\alpha = 0$ and $\lambda = 1$, ζ has the value 1 independently of the angle of incidence. This value corresponds to the speed of a homogeneous shear wave that is independent also of the parameter β. For $\lambda = 1.2$, the plots in Fig. 2c are mainly similar to those in Fig. 1c, except for $\alpha = 0.2$ for which ζ increases with θ initially, but then exhibits a maximum and thereafter decreases. For each value of θ except $\theta = 0$ the wave speed increases with the value of α. The effect of the coupling parameter α increases with increasing θ and, as in Fig. 1, is maximal for normal incidence. Comparison of the three panels in Fig. 2 highlights the effect of different values of λ.

To illustrate the dependence of the results on $\hat{D}_2$, ζ is plotted against $\hat{D}_2$ in Fig. 3 for $\lambda = 1.2$, $\beta = 0.2$ and four values of α in each of the three panels, which correspond to angles of incidence $\theta = \pi/16, \pi/4$ and $7\pi/16$ in the panels (a), (b) and (c), respectively. In Fig. 4 the roles are α and β are interchanged,
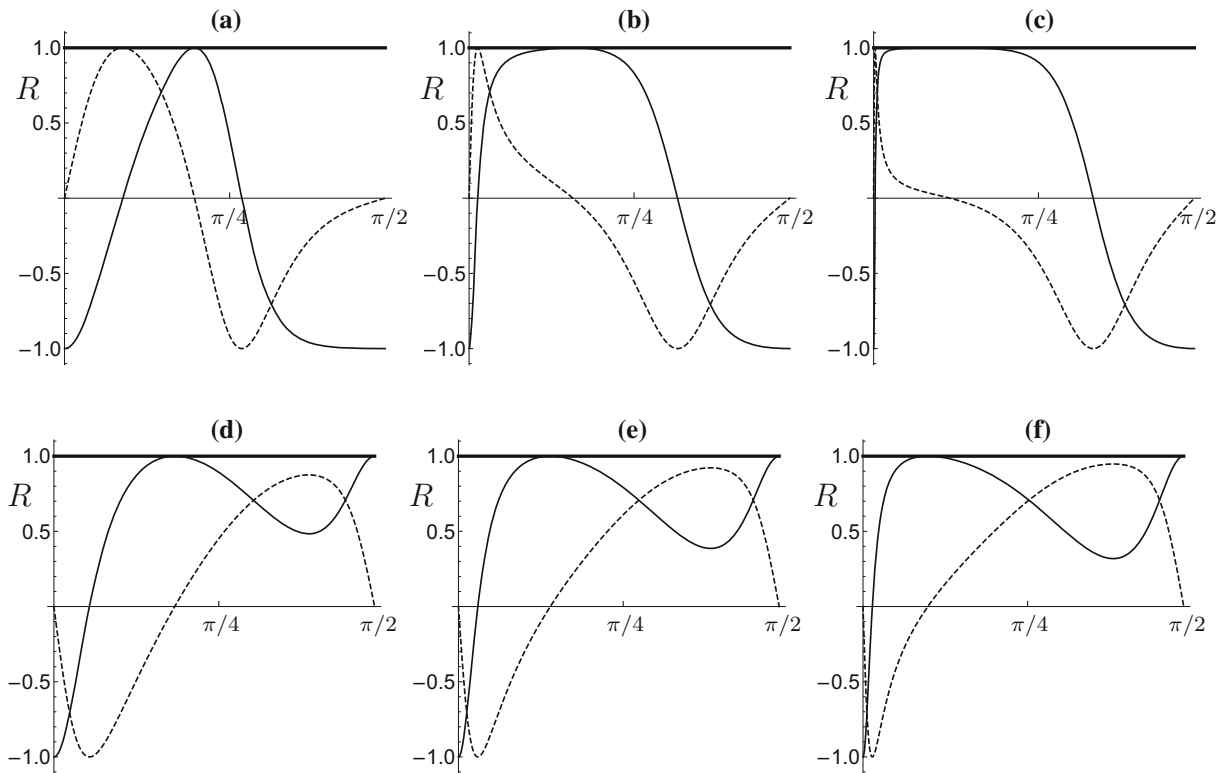
FIG. 10. Plots of $\mathrm{Re}(R)$, continuous curves, $\mathrm{Im}(R)$, dashed curves, and $|R| = 1$, versus $\theta \in [0, \pi/2]$ for $\lambda = 1.2$ with $\alpha = 0.1$: **a** $\beta = 0.1$, $\hat{D}_2 = 3$; **b** $\beta = 0.1$, $\hat{D}_2 = 5$; **c** $\beta = 0.1$, $\hat{D}_2 = 8$; **d** $\beta = 0.25$, $\hat{D}_2 = 3$; **e** $\beta = 0.25$, $\hat{D}_2 = 5$; **f** $\beta = 0.25$, $\hat{D}_2 = 8$

and the plots are for $\alpha = 0.1$ and four values of β, with the other parameters unchanged. Results for the other values of λ are qualitatively the same and are not therefore included separately. In each case (except for $\alpha = 0$) ζ increases monotonically with $\hat{D}_2$ and increases as the angle θ increases toward $\pi/2$. For $\alpha = 0$, ζ is independent of $\hat{D}_2$ and has a value that depends on θ. There is no effect of the coupling parameters α and β on the wave speed for $\hat{D}_2 = 0$, but for $\hat{D}_2 \neq 0$ ζ increases with α and/or β for each incident angle.

Figure 5 shows the dependence of R (a) and R' (b) on the angle of incidence θ for the basic case of $\lambda = 1$ with no dependence on the electric field. These results agree with those obtained for the purely elastic case [3] and are compared with corresponding results for the presence of an electric field in Figs. 6 and 7 (for $\lambda = 1$). In Fig. 6, the real and imaginary parts of R are shown together with $|R| = 1$ plotted against θ for $\alpha = 0.1$ and $\beta = 0.1$ (first row) and $\beta = 0.25$ (second row) with $\hat{D}_2 = 3, 5, 8$ in the first, second and third columns. This illustrates the dependence of R on the electric field (via $\hat{D}_2$) and electric parameters α and β subject to the restriction $\alpha + \beta < 0.5$. Note that $\mathrm{Re}(R) = -1$ and $\mathrm{Im}(R) = 0$ at the end points $\theta = 0, \pi/2$.

In Fig. 7 the real and imaginary parts of R' and $|R'|$ are plotted against θ for $\alpha = 0.1$ and $\beta = 0.1$ to illustrate the dependence on $\hat{D}_2$. The pattern is very similar for other values of α and β with some small differences in the vertical scale values. Note that $R' = 0$, i.e., there is no surface wave generated, at isolated values of the angle of incidence depending on the value of $\hat{D}_2$.

Figures 8 and 9 show further the dependence of the results on the value of $\hat{D}_2$. In Fig. 8 the real and imaginary parts of R and $|R| = 1$ are plotted against $\hat{D}_2$ for $\lambda = 1$, and the representative values
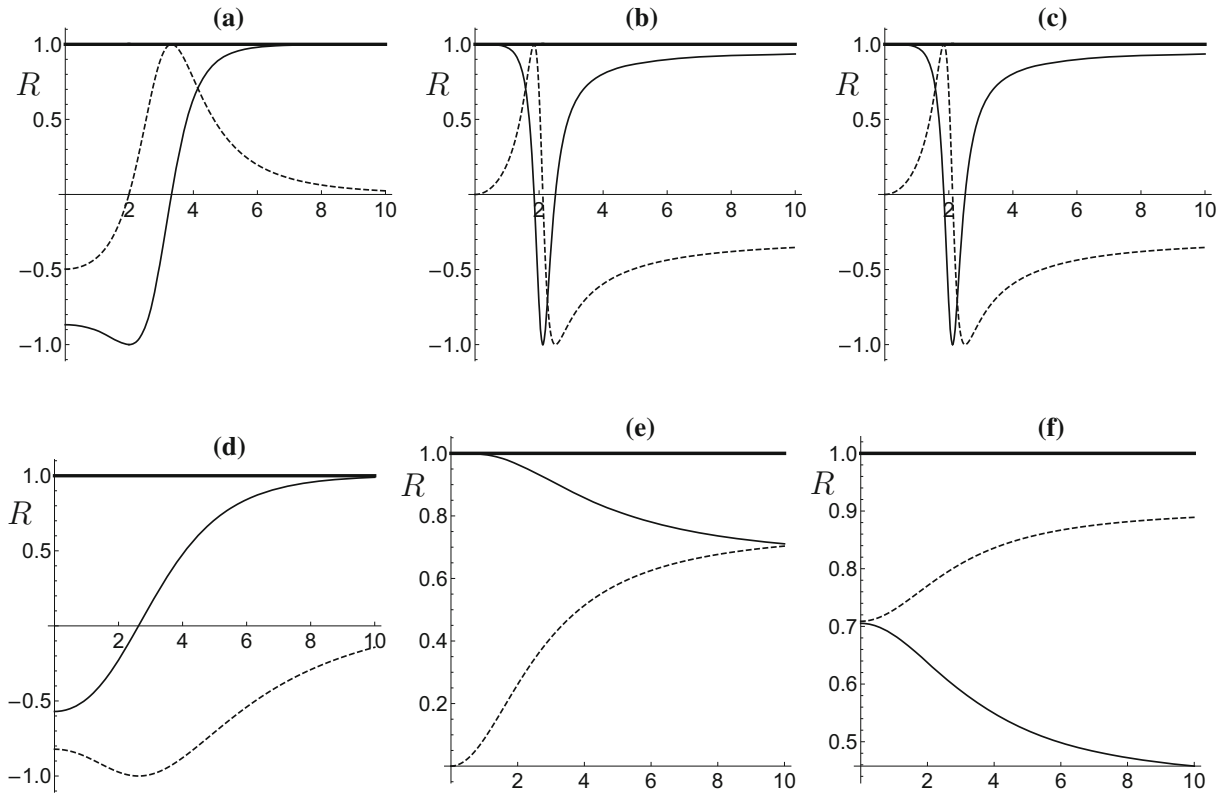
FIG. 11. Plots of Re(R), continuous curves, Im(R), dashed curves, and $|R| = 1$, versus $d \in [0, 10]$ for $\lambda = 1.2$, $\alpha = 0.1$ for different angles of incidence: **a** $\beta = 0.1$, $\theta = \pi/16$; **b** $\beta = 0.1$, $\theta = \pi/4$; **c** $\beta = 0.1$, $\theta = 7\pi/16$; **d** $\beta = 0.25$, $\theta = \pi/16$; **e** $\beta = 0.25$, $\theta = \pi/4$; **f** $\beta = 0.25$, $\theta = 7\pi/16$

$\alpha = \beta = 0.1$ for six different angles of incidence. Although not shown, it is clear that as $\theta \to \pi/2$, Re(R) $\to 1$ and Im(R) $\to 0$. In Fig. 9 the real and imaginary parts of R' and $|R'|$ are plotted against $\hat{D}_2$, again for $\lambda = 1$ and $\alpha = 0.1$, but $\beta = 0.2$, and with six different values of the angle of incidence chosen to illustrate the changing pattern.

Next, the dependence on the stretch λ is illustrated, specifically for $\lambda = 1.2$. In Figs. 10 and 11 the real and imaginary parts of R and $|R| = 1$ are plotted against θ and $\hat{D}_2$, respectively. With $\lambda = 1.2$ and $\alpha = 0.1$ in each case, the panels (a), (b), (c) in Fig. 10 are for $\beta = 0.1$, and panels (d), (e), (f) for $\beta = 0.25$ with $\hat{D}_2$ equal to 3, 5 and 8 in the three columns. The pattern can be compared with that for $\lambda = 1$ in Fig. 6. A key difference is that for the special case $\beta = 0.25$, $R = 1$ for $\theta = \pi/2$ compared with $R = -1$ in Fig. 6. The first row of Fig. 11, which shows the dependence of R on $\hat{D}_2$ for $\alpha = \beta = 0.1$ for specific angles of incidence, can likewise be compared with the appropriate panels in Fig. 7. The second row of Fig. 11 illustrates how the results change with the value of β.

Figure 12 shows the dependence of R' (real and imaginary parts and $|R'|$) on θ for $\lambda = 1.2$. The first row is for $\alpha = \beta = 0.1$ with $\hat{D}_2 = 3, 5, 8$ in panels (a), (b), (c), respectively. These plots can be compared directly with those in Fig. 8, the main differences being a reduction in the magnitude $|R'|$ and the change in sign of Im(R'). In panels (d) and (e), for $\hat{D}_2 = 3, 8$, respectively, $\beta = 0.3$ and the magnitude $|R'|$ has increased compared with that in panels (a) and (c). Finally, panel (f) considers the special value $\beta = 0.25$ for which R' has the value $\lambda^2/2\alpha$, in this case 7.2, at $\theta = \pi/2$. The final figure, Fig. 13, illustrates the
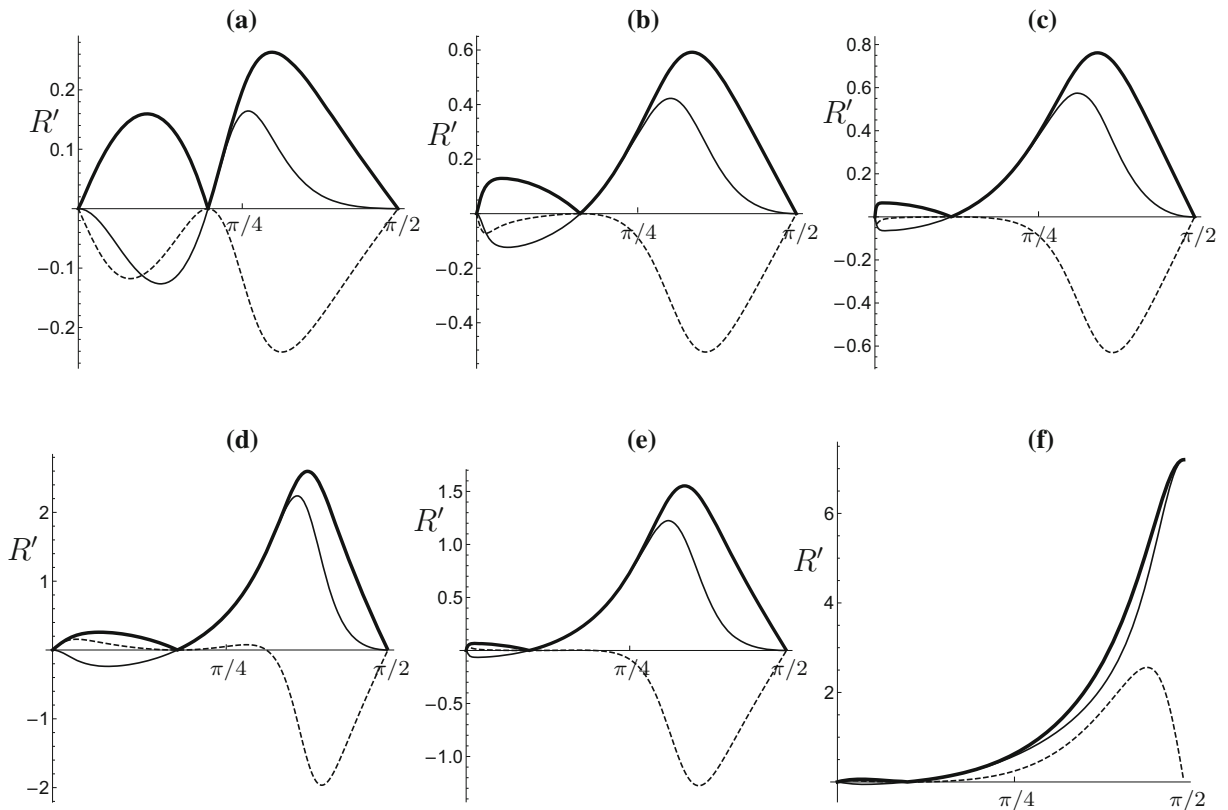
FIG. 12. Plots of $\mathrm{Re}(R')$, continuous curves, $\mathrm{Im}(R')$, dashed curves, and $|R'|$, thick continuous curves, versus θ for $\lambda = 1.2$, $\alpha = 0.1$: **a** $\beta = 0.1$, $\hat{D}_2 = 3$; **b** $\beta = 0.1$, $\hat{D}_2 = 5$; **c** $\beta = 0.1$, $\hat{D}_2 = 8$; **d** $\beta = 0.3$, $\hat{D}_2 = 3$; **e** $\beta = 0.3$, $\hat{D}_2 = 8$; **f** $\beta = 0.25$, $\hat{D}_2 = 8$

dependence of R' on $\hat{D}_2$ for $\lambda = 1.2$ and different values of the angle of incidence, the first row for $\alpha = \beta = 0.1$ and the second row for $\alpha = 0.1, \beta = 0.25$. The three columns are for $\theta = \pi/16, \pi/4, 7\pi/16$.

Results for other values of λ show similar patterns to those for $\lambda = 1.2$ and are not therefore included separately in order to save space.

9. Conclusions

This paper has provided a general summary of equations governing the quasi-electrostatic approximation for incremental electroelastic motions within a finitely deformed incompressible electroelastic material. Attention has then been focused on two-dimensional incremental motions and the propagation of plane incremental waves in a pure homogeneously deformed half-space of electroelastic material with an electric field normal to the boundary and for a simple prototype form of material model.

The dependence of the (dimensionless) squared speed of plane waves on the deformation (via the stretch λ), the electric coupling parameters α and β, and the (dimensionless) electric displacement field $\hat{D}_2$ has been illustrated in detail. One point to note is that when $\lambda = 1$ (no deformation) the wave speed is independent of the angle of propagation θ when $\alpha = 0$, and also independent of $\hat{D}_2$, as can be seen from Eq. (76). If, on the other hand, $\alpha \neq 0$ but $\beta = 0$ then the wave speed given by (73) is independent of $\hat{D}_2$, and independent of θ if $\lambda = 1$.
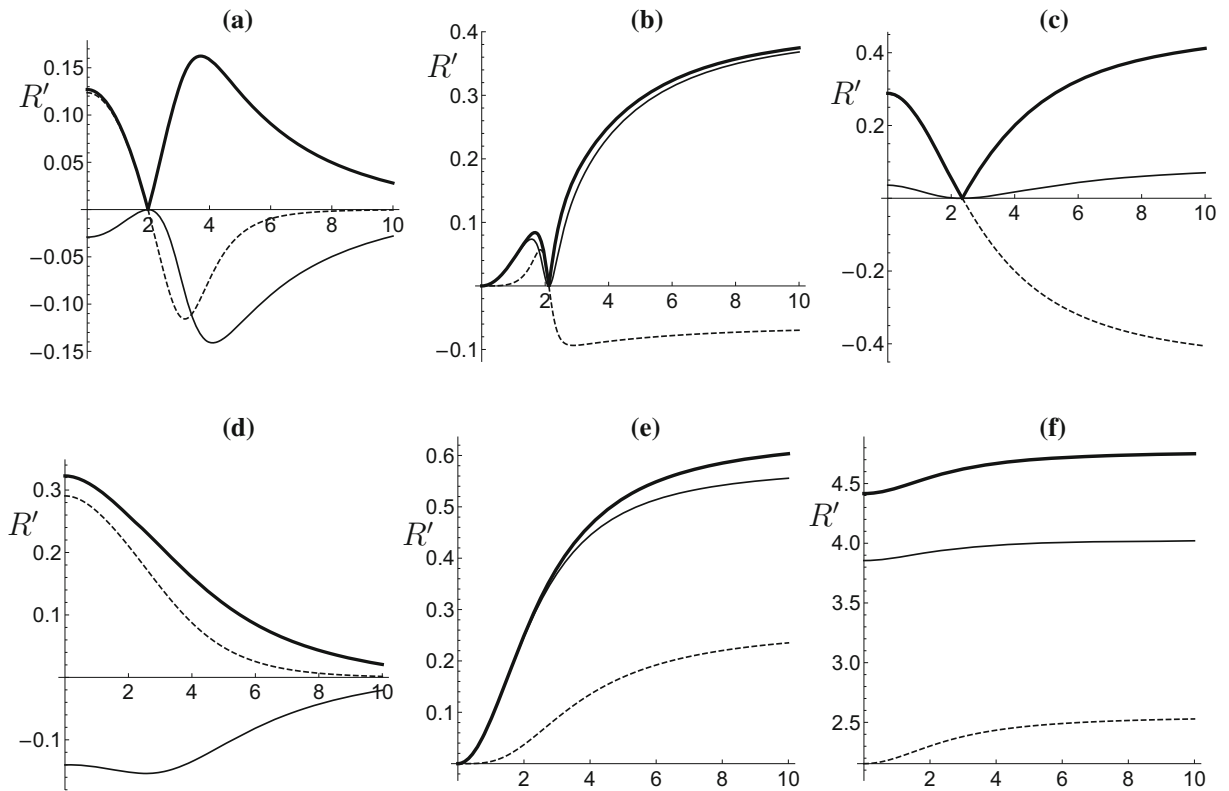
FIG. 13. Plots of Re(R'), continuous curves, Im(R'), dashed curves, and $|R'|$, thick continuous curves, versus $\hat{D}_2 \in [0, 10]$ for $\lambda = 1.2$, $\alpha = 0.1$ for different angles of incidence: **a** $\beta = 0.1$, $\theta = \pi/16$; **b** $\beta = 0.1$, $\theta = \pi/4$; **c** $\beta = 0.1$, $\theta = 7\pi/16$; **d** $\beta = 0.25$, $\theta = \pi/4$; **e** $\beta = 0.25$, $\theta = \pi/4$; **f** $\beta = 0.25$, $\theta = 7\pi/16$

In examining the reflection of plane waves impinging on a half-space boundary it has been shown that for the specific material model considered only one reflected wave is possible. This is in contrast to the purely elastic situation when a more general form of the elastic part of the model is adopted, as in [3]. The single reflected wave is in general accompanied by a generated surface wave. Expressions for the reflection coefficient R of the reflected wave are determined for the separate cases of an undeformed and deformed half-space, with their dependence on α, β and $\hat{D}_2$, and the differences in these two cases have been highlighted. The corresponding coefficient R' of the surface wave has also been obtained and its features examined similarly. Both R and R' are affected significantly by the parameters λ, α, β and $\hat{D}_2$.

Acknowledgements

References

[1] Dorfmann, A., Ogden, R.W.: Nonlinear electroelasticity. Acta Mech. **174**, 167–183 (2005)
[2] Dorfmann, A., Ogden, R.W.: Electroactive waves in a finitely deformed electroactive material. IMA J. Appl. Math. **75**, 630–636 (2010a)
[3] Ogden, R.W., Sotiropoulos, D.A.: The effect of pre-stress on the propagation and reflection of plane waves in incompressible elastic solids. IMA J. Appl. Math. **59**, 95–121 (1997)
[4] Liu, H., Kuang, Z.B., Cai, Z.M.: Propagation of Bleustein–Gulyaev waves in a prestressed layered piezoelectric structure. Ultrasonics **41**, 397–405 (2003)
[5] Simionescu-Panait, O.: Wave propagation in cubic crystals subject to initial mechanical and electric fields. Z. Angew. Math. Phys. **53**, 1038–1051 (2002)
[6] Singh, B.: Wave propagation in a prestressed piezoelectric half-space. Acta Mech. **211**, 337–344 (2009)
[7] Yang, J.S., Hu, Y.: Mechanics of electroelastic bodies under biasing fields. Appl. Mech. Rev. **57**, 173–189 (2004)
[8] Ogden, R.W.: Non-linear Elastic Deformations. Dover, New York (1997)
[9] Dorfmann, L., Ogden, R.W.: Nonlinear Theory of Electroelastic and Magnetoelastic Interactions. Springer, New York (2014)
[10] Jackson, J.D.: Classical Electrodynamics. Wiley, New York (1999)

Baljeet Singh
Department of Mathematics
Postgraduate Government College
Sector 11
Chandigarh 160011
India

Ray W. Ogden
School of Mathematics and Statistics
University of Glasgow
Glasgow
UK
e-mail: raymond.ogden@glasgow.ac.uk